JOURNAL OF APPLIED METEOROLOGY

March, 1975, p.252

Broadband Antenna Systems for Lightning Magnetic Fields

E. PHILIP KRIDER AND R. CARL NOGGLE

Institute of Atmospheric Physics, The University of Arizona, Tucson 85721

12 June 1974 and 11 November 1974

ABSTRACT

Broadband magnetic field antenna systems which can resolve submicrosecond structure in lightning waveforms are described. Correlated data on the magnetic and electric fields produced by distant lightning are presented and are shown to be, for the most part, identical in shape.

1. Introduction

Recent broadband measurements of electric fields produced by lightning show return stroke waveforms with microsecond and occasionally submicrosecond initial risetimes (Fisher and Uman, 1972; Uman *et al.*, 1973a; Lin and Uman, 1973) and intracloud discharge signals which are often faster. Uman and co-workers have developed a general theoretical description production of electric fields by return strokes (McLain and Uman, 1971) and also a model which, when the model assumptions are met, can be used to infer channel currents from absolute measurements of electric field waveforms (Uman *et al.*, 1973b). Uman and McLain (1969, 1970) have also developed a similar theory and a model for the production of magnetic fields, but until now no measuring system was available with sufficient bandwidth to resolve the detailed structure of return stroke waveforms, and hence no adequate magnetic field records have been obtained.

In this note, we describe broadband magnetic antenna systems suitable for recording submicrosecond field changes and present typical data from distant lightning. The shapes of simultaneous electric and magnetic fields will be presented and will be shown to be, for the most part, identical.

2. Antenna system

Schematic diagrams of two types of broadband magnetic field antennas are shown in Figs. 1 and 2. In each case, the basic detector element is a single turn shielded loop antenna. The voltage induced in the antenna loop is proportional to the time-derivative of the external magnetic flux density, *dB/dt*, and a geometrical factor which depends on the loop area and the angle to the discharge. A signal proportional to *B* is obtained by electronically integrating the differential antenna output over time. In both cases, the antennas were remote from the building housing the integrating electronics and recording oscilloscope to minimize distortions in the lightning magnetic fields near the antenna.

The antenna shown in Fig. 1 was constructed of 0.1-mm diameter copper wire centered inside a 1.0 m^2 electric shield made of 53-mm i.d. aluminum pipe with a wall thickness of 3 mm. With these dimensions, the characteristic impedance of the antenna was about 400Ω. A battery-powered differential follower located in the antenna base acted as an impedance transformer for transmission of the *dB/dt* signals from the antenna to the differential integrator through coaxial cables. The follower was usually set for a gain of 2, but, for very distant lightning, improved performance could be obtained by increasing the follower gain at the expense of some reduction in bandwidth. The antenna was terminated in its characteristic impedance at both inputs to

the differential follower, to prevent any overshoot or ringing in the *dB/dt* waveform. The shield was discontinuous at the top of the antenna to prevent induced currents from flowing in the shield loop. Any electric field transients or 60-Hz background detected at the separation of the shield appeared equally on both signal inputs and were rejected by the integrator as a common-mode signal.

A twisted pair of coaxial cables inside 18-mm diameter copper braid conducted the antenna outputs to the integrator. Any magnetic transients induced on the signal cables by lightning or a 60-Hz background were equal and were rejected by the differential integrator. The braid was connected to the loop shield, and all electronic grounds were isolated from the shield except at one point on the integrator chassis.

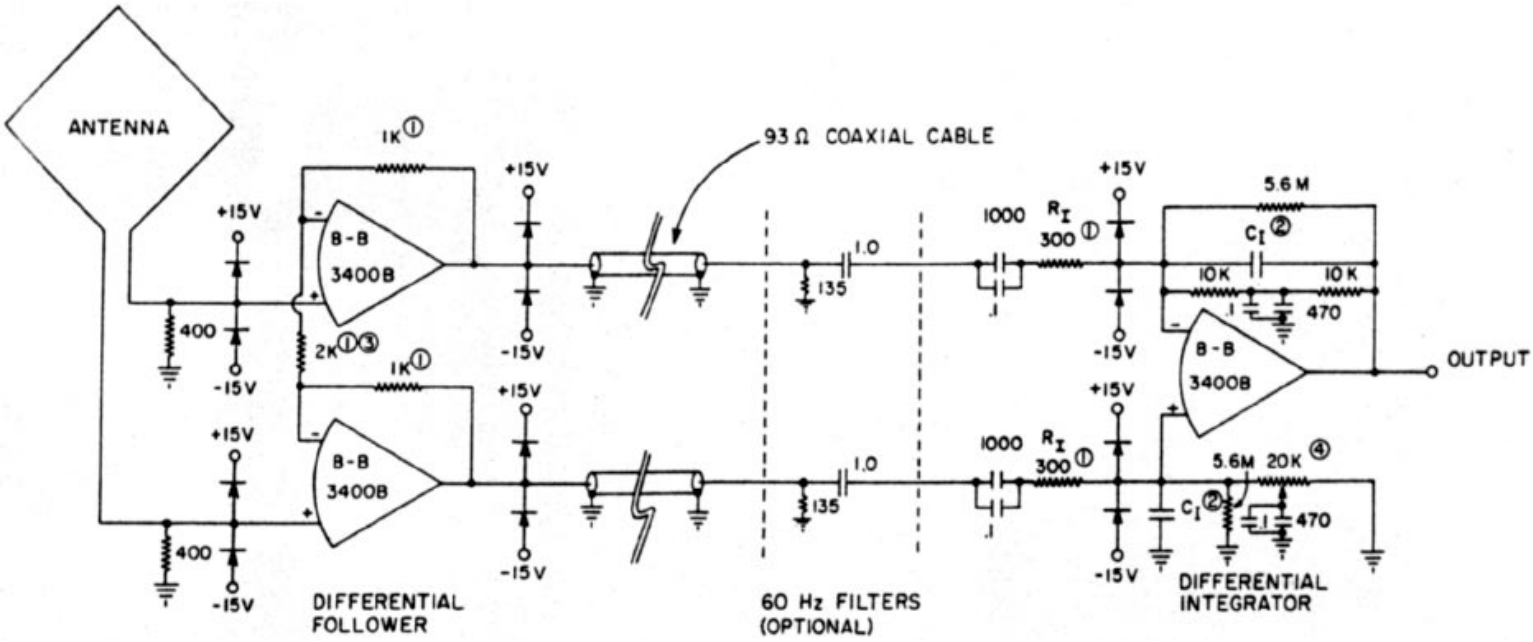

NOTES:
1) 1% NONINDUCTIVE RESISTORS
2) LOW-LOSS 1% CAPACITORS - 100 TO 10,000 pF
3) THIS RESISTOR CAN BE REDUCED TO 200Ω TO PROVIDE A FOLLOWER GAIN OF 11.
4) ADJUST FOR OPTIMUM COMMON MODE REJECTION

ALL DIODES 1N4447
ALL CAPACITOR VALUES IN μF

Fig. 1. A schematic diagram of a high-impedance magnetic field antenna and associated electronics.

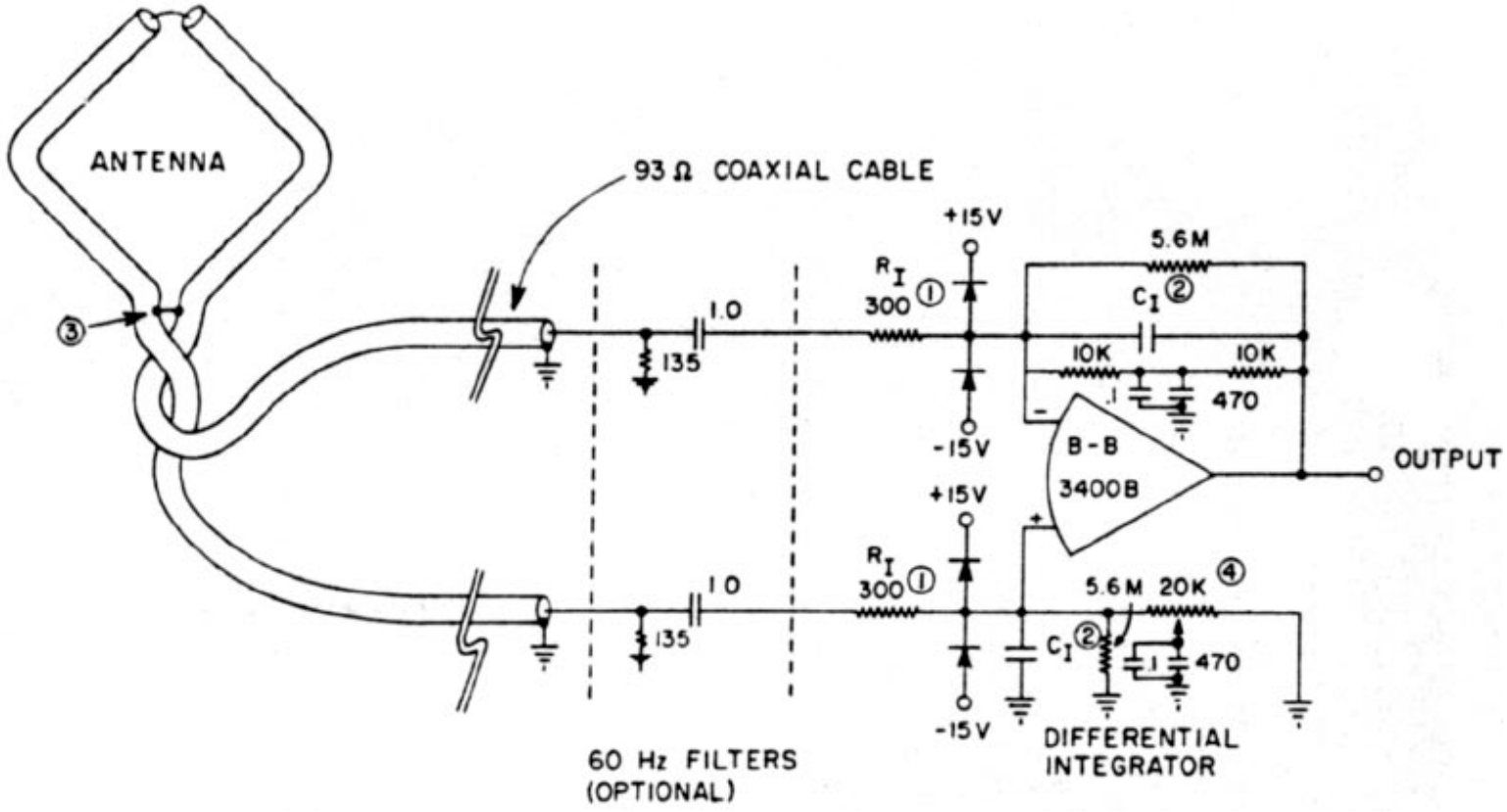

NOTES:
1) 1% NONINDUCTIVE RESISTORS
2) LOW-LOSS 1% CAPACITORS - 100 TO 10,000 pF
3) OUTSIDE COAX SHIELDS CONNECTED HERE
4) ADJUST FOR OPTIMUM COMMON MODE REJECTION
ALL DIODES 1N4447
ALL CAPACITOR VALUES IN μF

Fig. 2. A schematic of a magnetic field antenna formed from a single loop of 93Ω coaxial cable and associated electronics.

Fig. 2 shows a schematic of an antenna system in which both the antenna loop and twisted signal leads are formed from a single piece of coaxial cable. This construction has the advantage that the differential follower at the antenna base can be omitted if the signal cables are terminated properly at the integrator inputs. As we shall see, the lower impedance of a coaxial cable loop results in a reduced antenna output at high frequencies, but the response is still adequate for most lightning applications.

The differential follower and differential integrators were constructed from Burr-Brown 3400B operational amplifiers, as shown in Figs. 1 and 2. These amplifiers have a slew rate of 1000 V μs^{-1}, a gain-bandwidth product of 100 MHz, fast settling, and low drift. All resistors and capacitors used in the differential signal circuits were carefully matched, and fast diodes were used to protect all amplifiers from excessive transients.

Figs. 1 and 2 show single-stage RC filters before the differential integrator inputs. These were used to reduce unwanted 60 Hz and can be increased or eliminated depending on the background level. The integrator inputs in Fig. 1 were always ac coupled, to prevent unwanted variations in the integrator output level due to drifts in the differential follower outputs. When using a coaxial cable antenna, the integrator cam be dc coupled.

The integrator output voltage V is related to the incident magnetic flux density B (Wb m^{-2}) by

$$V = \frac{KA\ cos\phi}{R_I C_I} B \quad (1)$$

where K is the gain of the differential follower, A the antenna area (m^2), ϕ the angle between the plane of the loop and the lightning discharge, and R_I and C_I the integrating resistance and capacitance. Normally R_I was fixed at 300Ω and C_I could be varied from 10^{-4} to 10^{-2} μF, to provide different output levels. The input impedance of the integrator, which is determined by R_I and the resistors to ground terminating the signal cables, should always match the characteristic impedance of the signal cables. A high-pass filter in the integrator feedback loop provided dc stabilization of the integrator output. The common-mode rejection of the differential integrator was optimized by adjusting the 20-kΩ potentiometer for minimum output when identical square test signals were applied to both. inputs.

The response of an antenna to fast and slow signals was tested by applying a known current pulse to a small transmitting loop located near the antenna, the test magnetic field having the same shape as the current pulse. Fig. 3 shows an input test waveform and the outputs of two 1 m^2 antenna systems. The 400Ω antenna with differential follower provided the fastest risetime (10% to 90%), about 33 ns, and was limited primarily by the gain-bandwidth product of the differential follower and the slew rate and maximum output current of the amplifiers. The 50Ω cable antenna had a risetime of 88 ns, which was primarily due to the larger current induced in the antenna loop, generating a magnetic field proportional to dB/dt in opposition to the incident field. This effect can be reduced by using higher impedance cable or a smaller area antenna loop. The 93Ω antenna shown in Fig. 2 had a risetime of about 37 ns, and a 93Ω loop (20 cm X 20 cm) had a risetime of about 20 ns, the limit of the integrator electronics. With a C_I of 1000 pF, the decay time constants of the antenna systems were about 4 ms without the 60-Hz filters and 1.3 ms when they were included. Without the filters, the decay time constant is primarily determined by the product of C_I and the parallel 5.6 MΩ resistor.

The antennas were tested for immunity to external electric fields by placing them under a large copper screen to which fast high-voltage pulses were applied. When the antennas were located under the center of the screen, no electric field signals could be detected in a field of 5000 V m^{-1} using 100-pF integrating capacitors. If the antennas were not located symmetrically under the screen, a small magnetic signal was detected which was proportional to the applied dE/dt signal.

In a typical experiment, the magnetic field signals were delayed and then photographed on an oscilloscope using a 35-mm camera with continuously moving film to separate the different components in a lightning flash. The oscilloscope was triggered on the initial portion of the magnetic waveform by amplifying the time-derivative of the absolute value of the integrator output.

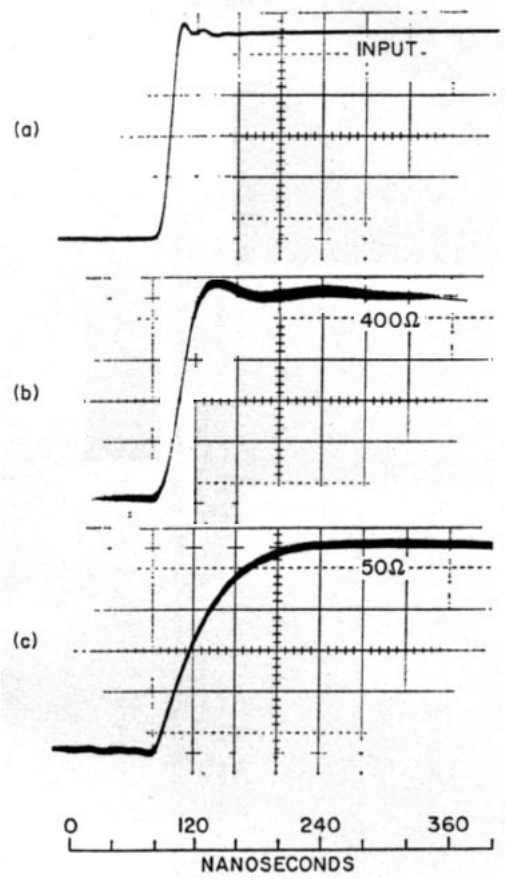

Fig. 3. An input magnetic field test waveform (a), and the relative responses of 1 m^2 antenna systems. The output of a 400Ω system with differential follower is shown in (b), and the output of a 50Ω cable system in (c).

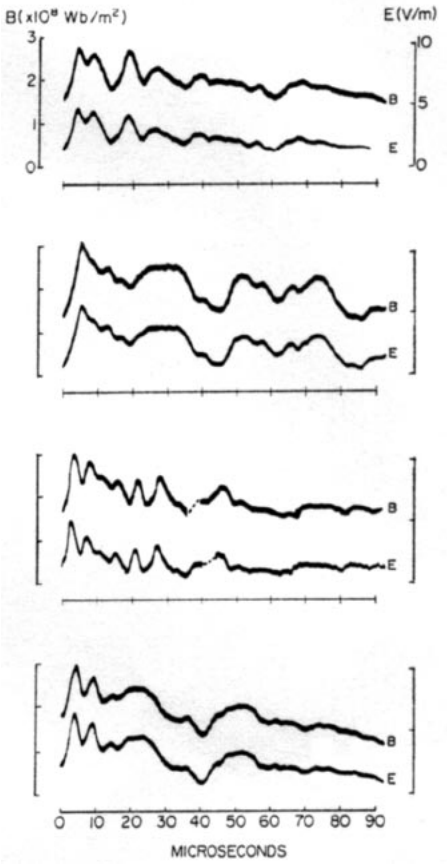

Fig. 4. Correlated magnetic (*B*) and electric (*E*) field waveforms from lightning at a distance of 50-100 km. The same vertical scales apply to all records.

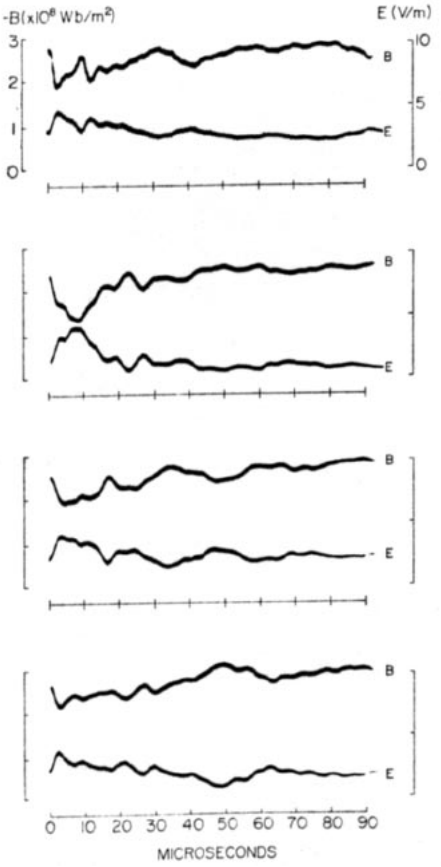

Fig. 5. Correlated magnetic (*B*) and electric (*E*) field waveforms from lightning at a distance of 50-100 km The magnetic fields are inverted with respect to the electric because ø in Eq. (1) was close to π

3. Data

Figs. 4 and 5 show examples of typical lightning magnetic field waveforms, which were obtained at distances of 50 to 100 km and which have shapes typical of return strokes. Also shown are correlated electric field records obtained using a calibrated antenna similar to that described by Fisher and Uman (1972). These data were recorded using 2.5-μs delay lines which had a risetime of 0.2-μs. To our knowledge, the data in Figs. 4 and 5 represent the first correlated broadband electric and magnetic field waveforms which have been published for lightning.

For the data shown in these figures, the antenna was oriented such that the magnetic-field signals were close to a maximum. From Eq. (1), the incident magnetic flux density is related to the integrator output voltage V by

$$B = \frac{R_I C_I V}{KA \cos\phi} \qquad (2)$$

This relation was checked and found to be accurate to within 10% by comparing magnetic field values with the calibrated electric field measurements. When the largest magnetic signals were received relative to the electric (ø=0), the ratio of the radiation field intensities was found to be $E/B=c$, where c is the speed of light, a general relation predicted by theory (McLain and Uman, 1971). For more precise work two orthogonal antenna loops can be used to obtain the total magnetic field vector.

As can be seen, the shapes of distant electric and magnetic fields are almost identical, as expected for radiation fields. The initial field risetimes are typically 1-5 μs and are distributed in a fashion similar to those of Lin and Uman (1973). The shapes of the distant magnetic fields after the initial rise agree quite well with the pioneering results of Norinder and co-workers (1945, l956), the only previously published broadband measurements.

In a subsequent paper, we will describe an accurate lightning direction finder which employs an orthogonal pair of broadband magnetic antennas similar to those described above. Accurate directions are obtained even for close lightning by gating the signals, such that the incident magnetic field vectors are sampled at only those times when the return stroke currents are close to the ground.

Acknowledgments. We are grateful to Dr. Martin A. Uman at the University of Florida for numerous, helpful discussions and to G. J. Radda for assistance in obtaining the data. This work was supported in part by the Atmospheric Sciences Section of the Office of Naval Research, Contract N00014-67A-0209-0015, and the NASA Kennedy Space Center.

REFERENCES

Fisher, R. J., and M. A. Uman, 1972: Measured electric field rise times for first and subsequent lightning return strokes. *J. Geophys. Res.*, **77**, 399-406.

Lin, Y. T., and M. A. Uman, 1973: Electric radiation fields of lightning return strokes in three isolated Florida thunderstorms. *J. Geophys. Res.*, **78**, 7911-7915.

McLain, D. K., and M. A. Uman, 1971: Exact expression and moment approximation for the electric field intensity of the lightning return stroke. *J. Geophys. Res.*, **76**, 2101-2105.

Norinder, H., 1956: Magnetic field variations from lightning strokes in the vicinity of thunderstorms. *Ark. Geofys.*, **2**, 423-451.
—, and O. Dahle, 1945: Measurements by frame aerials of current variations in lightning discharges. *Ark. Mat. Astron. Fys.*, **32A**, 1-70.

Uman, M. A., and D. K. McLain, 1969: Magnetic field of lightning return strokes. *J. Geophys. Res.*, **74**, 6899-6910.
—, and —, 1970: Lightning return stroke current from magnetic and radiation field measurements. *J. Geophys. Res.*, **75**, 5143-5147.
—,—, R. J. Fisher and E. P. Krider, 1973a: Electric field intensity of the lightning return stroke. *J. Geophys. Res.*, **78**, 3523-3529.
—,—,—, and —, 1973b: Currents in Florida lightning return strokes. *J. Geophys. Res.*, **78**, 3530-3537.